PERGAMON

Chemical Engineering Science 58 (2003) 115–133

Chemical Engineering Science

www.elsevier.com/locate/ces

Evolution of hydrodynamic and statistical parameters of gas–liquid slug flow along inclined pipes

R. van Hout*, L. Shemer, D. Barnea

Department of Fluid Mechanics and Heat Transfer, Faculty of Engineering, Tel-Aviv University, 69978 Tel-Aviv, Israel

Received 24 October 2001; received in revised form 6 May 2002; accepted 10 September 2002

Abstract

The development of slug flow along two 10 m long inclined pipes (2–90° from the horizontal) with internal diameters of 0.024 and 0.054 m was measured by three optical fiber probes. The probes were located in a measurement module at axial distances of 0.020 m between the fiber tips. To measure the evolution of slug flow, the module was placed at different positions along the pipe. Instantaneous elongated bubble velocities and corresponding elongated bubble and liquid slug lengths were determined by processing the optical probe signals. The evolution of the liquid slug and elongated bubble length distributions along the pipes is characterized by a gradual growth of the mean and mode values. The growth rate decreases with decreasing inclination. Mean elongated bubble lengths have a minimum at about 60°, while mean liquid slug lengths decrease slowly with decreasing inclination angle. The coalescence rate, defined as the decrease in the ensemble size, becomes almost negligible at $x/D > 60$, independent of pipe diameter, flow rates and inclination angle. The slug frequency has a maximum at about 60° inclination.

Keywords: Multiphase flow; Evolution of gas–liquid slug flow; Inclined pipes; Length distributions; Slug frequency

1. Introduction

Gas–liquid two phase slug flow is one of the most complex flow patterns since it is intrinsically unsteady. In inclined slug flow, liquid slugs filling the whole cross-section of the pipe are separated by a stratified zone with an elongated bubble in the upper part of the pipe. The liquid slugs may be aerated with small gas bubbles.

The evolution of slug flow along a pipeline strongly depends on the relative velocities between the elongated bubbles. At small separation distances, trailing elongated bubbles accelerate and eventually merge with the leading ones (Moissis & Griffith, 1962; Pinto & Campos, 1996; Pinto, Coelho Pinheiro, & Campos, 1998; Fagundes Netto, Fabre, Grenier, & Péresson, 1998; Aladjem Talvy, Shemer, & Barnea, 2000). During the merging process, both the liquid slug and the elongated bubble lengths increase. This process is assumed to terminate once the liquid velocity profiles at the back of the liquid slug are fully developed and all elongated bubbles propagate at the same translational velocity.

Nicklin, Wilkes, and Davidson (1962) proposed a correlation for the calculation of the translational velocity of an elongated bubble in continuous slug flow

$$U_{\mathrm{Nick}} = CU_m + U_d, \tag{1}$$

where U_d is the drift velocity of the bubble in a stagnant liquid, and U_m is the mixture velocity defined as the sum of the liquid and gas superficial velocities, U_{LS} and U_{GS}. The value of the constant C is based upon the assumption that the propagation velocity of the bubbles follows the maximum local velocity, $U_{\max}$, in front of the nose tip and thus $C = U_{\max}/U_m$ (Nicklin et al., 1962; Bendiksen, 1984; Shemer & Barnea, 1987; Polonsky, Shemer, & Barnea, 1999). The value of C therefore equals approximately 1.2 for fully developed turbulent flow and 2.0 for fully developed laminar flow.

The drift velocity U_d depends on the inclination angle β, measured from the horizontal, and has a maximum for $40° < \beta < 60°$ (Zukoski, 1966; Bendiksen, 1984; Hasan & Kabir, 1986; Weber, Alarie, & Ryan, 1986; Fabre & Liné, 1992; Carew, Thomas, & Johnson, 1995; van Hout, Barnea,

* Corresponding author. Present address: Department of Mechanical Engineering, Whiting School of Engineering, Johns Hopkins University, 200 Latrobe Hall/3400 N. Charles Street, Baltimore, MD 21218-2686, USA. Tel.: +1-410-516-5427; fax: +1-410-516-7254.

E-mail address: vanhout@pegasus.me.jhu.edu (R. van Hout).

0009-2509/02/$ - see front matter © 2002 Elsevier Science Ltd. All rights reserved.
PII: S0009-2509(02)00441-4

& Shemer, 2002). Furthermore, U_d increases with decreasing surface tension parameter $\Sigma = 4\sigma/\Delta\rho g D^2$ (Zukoski, 1966), where g is the gravitational constant, D the pipe diameter, σ the surface tension and $\Delta\rho$ the density difference between the liquid and the gas phases. For inclined flows, U_d has been correlated by Bendiksen (1984) as a weighted superposition of the drift velocity in a vertical pipe, U_d^v, and in a horizontal pipe, U_d^h

$$U_d(\Sigma,\beta) = U_d^h(\Sigma,\alpha_B)\cos\beta + U_d^v(\Sigma,\alpha_B)\sin\beta, \qquad (2)$$

where α_B is the void fraction in the film region of the elongated bubble. The drift velocities U_d^v and U_d^h depend on the surface tension parameter Σ (van Hout et al., 2002). Limiting values of U_d for negligible $\Sigma(<0.001)$ were determined by Dumitrescu (1943) for the vertical case, $U_d^v = 0.35\sqrt{gD}$, and by Benjamin (1968) for the horizontal case, $U_d^h = 0.54\sqrt{gD}$.

Most experimental research in developed slug flow concerning length distributions has been focused on determining the mean and maximum liquid slug lengths. Mean liquid slug lengths $\langle \ell_s \rangle$ (measured in pipe diameters D) were found to be relatively independent of flow rates. Measured normalized mean liquid slug lengths for vertical flow lie in the range from 10 to 20D with standard deviations between 30% and 50% (Griffith & Wallis, 1961; Barnea & Shemer, 1989; van Hout, Shemer, & Barnea, 1992; Nydal, Pintus, & Andreussi, 1992; Costigan & Whalley, 1997; van Hout, Barnea, & Shemer, 2001). Felizola and Shoham (1995) found for inclined air–kerosene slug flow that $\langle \ell_s \rangle$, averaged over all investigated flow rates, has a minimum of about 16D at $\beta = 60°$. For the horizontal case, reported mean liquid slug lengths vary between 10 and 100D (Nicholson, Aziz, & Gregory, 1978; Nydal et al., 1992; Andreussi, Bendiksen, & Nydal,1993; Felizola & Shoham, 1995). Maximum lengths have been reported to be 2–3 times the mean lengths.

Experimental measurements of the liquid slug and elongated bubble length distributions have been carried out mainly for horizontal or slightly inclined slug flow and for vertical flow. The liquid slug length distribution can be described by positively skewed distributions, such as the log-normal, the gamma, or the inverse Gaussian (Brill, Schmidt, Coberly, Herring, & Moore, 1981; Dhulesia, Bernicot, & Deheuvels, 1991; Nydal et al., 1992; van Hout et al., 2001). Modeling of the evolution of slug flow was undertaken by Bernicot and Drouffe (1989) for the horizontal case and by Barnea and Taitel (1993) for all inclination angles. The latter model was verified against experimental data for the slightly inclined case by Cook & Behnia (2000) and for the vertical case by Hasanein et al. (1996) and van Hout et al. (2001). Model predictions compared reasonably well with the experimental data. The dependency of the elongated bubble translational velocity on the liquid slug length ahead of it, $U_t = f(\ell_s)$, should be provided as an input relation to the Barnea and Taitel model.

The aim of the present investigation is to study experimentally the evolution of various hydrodynamic and statistical parameters of slug flow along inclined pipes. Parameters such as liquid slug and elongated bubble length distributions, as well as the elongated bubble translational velocities were determined at various locations along the pipe. Furthermore, the dependency of the instantaneous elongated bubble nose velocity on the liquid slug length ahead of it was measured for inclined continuous slug flow. This information is essential for developing reliable models for the prediction of the evolution of slug length distributions.

2. Description of the experiment

2.1. Experimental facility

The experimental facility consists of two 10 m long, parallel transparent Perspex pipes which have internal diameters of 0.024 and 0.054 m. The system can be rotated around its axis and fixed at any inclination angle from horizontal to vertical.

The gas and the liquid superficial velocities are measured by a set of rotameters. Air is supplied from a central line via a pressure reducer adjusted to 0.1 Mpag within the rotameter. The inlet valve used to adjust the gas flow rate is located downstream of the rotameter. The test pipes are open to the atmospheric pressure at the exit and the volumetric gas flow rate measured by the rotameters is converted to standard atmospheric conditions. The gas flow rates presented in the following figures relate to the conditions prevailing at the exit. Since the gas superficial velocity increases along the pipe due to gas expansion, the effective gas superficial velocity at the measurement position was recalculated by taking into account the pressure drop along the pipe (Barnea, 1990). The mixture velocity at the measurement position U_m in Eq. (1), was adjusted accordingly.

Tap water filtered by an ion exchanger is circulated through the system in a closed loop by a centrifugal pump. The two fluids were introduced through a "mixer"-type inlet device with a length of 30 cm. More details on the experimental facility can be found in van Hout et al. (2001).

2.2. Measurement methods and data processing

Experiments were carried out in upward inclined co-current slug flow using mainly optical fiber probes that detect the local instantaneous phase at their tip (i.e. gas or liquid). Three probes were mounted on a specially constructed measurement module at an axial distance of 0.020 m between adjacent probes (van Hout et al., 2001). A traversing mechanism (unislide) allowed accurate positioning of the probe tips at any radial location inside the pipe. The evolution of slug flow along the pipe was measured by placing the measurement module at different positions x/D along the pipe, where x is the axial pipe coordinate measured from the inlet section.

The return signals of the optical probes were sampled by an A/D converter at a sampling frequency of 1 kHz and a sampling duration of 3600 s. The typical number of slug units measured continuously at any given flow condition was of the order of 10^3. The sampled optical probe signals essentially represent the residence time history of the two phases at the probe tips. Instantaneous propagation velocities, U_{inst}, of each elongated bubble nose or tail interface were determined by the time interval required for the interface to move from one probe to the other. The elongated bubble lengths were determined by multiplying the residence time of the gas bubble over the probe tip by the bubble nose velocity. The liquid slug lengths ahead of the bubble were then calculated by multiplying the residence time of the liquid slug with the instantaneous velocity of the preceding elongated bubble tail. Thus, the dependency between the instantaneous elongated bubble velocity and the liquid slug length in front of it, $U_{\text{inst}} = f(\ell_s)$ was determined. In addition, characteristic translational velocities at different measurement positions and inclination angles were determined by cross-correlating two consecutive probe signals, taking advantage of the coherency of the signals between neighboring probes. A comprehensive description of the data processing can be found in van Hout et al. (2001).

An image processing technique was used to validate the results obtained by the optical probes. Series of images of the flow taken by a camera were digitized by a frame-grabber board and then processed. Typical ensemble sizes were of the order of few tens. The major advantage of image processing over the optical probes is the direct extraction of lengths and velocities from the images (van Hout et al., 2002). However, the use of image processing in continuous slug flow is limited since elongated bubble interfaces are hard to detect due to the highly aerated liquid slug region and the bubble's fierce oscillations.

2.3. Experimental conditions

The evolution of slug flow along the pipes was investigated for a wide range of inclinations ($2^\circ < \beta < 90^\circ$) and flow rates ranging from $U_m = 0.22$ to 0.73 m/s. The Reynolds number, $Re = U_m D/\nu$, ranges between $10,000 < Re < 40,000$ based on the liquid kinematic viscosity. For 90° upward flow, the optical probes were mounted at the centerline of the pipes, while for inclined flow the probe tips were located in the upper part of the pipe, for $D = 0.054$ m at $y = 6.5$ mm and for $D = 0.024$ m at $y = 6$ mm, where y is measured from the upper wall of the pipe. The silica probe fiber extended 10 mm from the stainless-steel probe body with a sensitive probe tip diameter of 0.14 mm minimizing intrusive effects.

The camera and halogen lighting were mounted on a specially constructed aluminum frame that was fixed to the steel frame of the experimental facility. The camera was located at 7.9 m from the pipe inlet, corresponding to $x/D = 146$ for $D = 0.054$ m and $x/D = 329$ for $D = 0.024$ m.

3. Experimental results

3.1. Evolution of the characteristic elongated bubble velocities along the pipe

The normalized measured characteristic velocities of elongated bubbles U_t according to the cross-correlation technique, at various locations along both pipes are presented in Fig. 1 for different pipe inclinations. The velocities measured by the optical probes were validated by image processing technique (van Hout et al., 2002). The values of U_t are normalized by U_{Nick}, Eq. (1), using $C = 1.2$ and U_d according to Eq. (2). In the present study the drift velocity in vertical pipes is not affected by the surface tension and U_d^v was calculated according to Dumitrescu (1943). For the horizontal case, the drift velocity, U_d^h, was taken at the appropriate surface tension parameter (Zukoski, 1966; van Hout et al., 2002), yielding $U_d^h = 0.18$ m/s for $D = 0.024$ m, and $U_d^h = 0.33$ m/s for $D = 0.054$ m. The values of U_{Nick} at different positions along the pipe were calculated by taking gas expansion into account (van Hout et al., 2001) and are presented in Table 1.

The normalized velocities (Fig. 1) are characterized by increased values near the pipe inlet due to the undeveloped nature of the flow. Further down the pipe the normalized velocities decrease to a more or less constant value. For the small pipe diameter, Figs. 1(b) and (d), the translational velocities near the pipe exit approach the value given by Eq. (1), being within 10% of U_{Nick} for both flow rates. In contrast to this for $D = 0.054$ m, the measured velocities at the pipe exit are underpredicted by Eq. (1) for $\beta > 10^\circ$. This discrepancy increases with the inclination angle β and can be attributed to the absorption of small, dispersed bubbles at the elongated bubble nose resulting in an effectively higher translational velocity (van Hout et al., 2002).

3.2. Liquid slug and elongated bubble length distributions

The most precise way of determining the length distributions from the measured residence times is by using the instantaneous propagation velocity of nose or tail, U_{inst}, of each bubble separately.

The ensemble-averaged instantaneous translational velocities of a trailing bubble nose as a function of the separation distance, $\langle U_{\text{inst}} \rangle = f(\ell_s)$, are presented in Figs. 2 and 3 at different locations along the pipe for $D = 0.024$ and 0.054 m, respectively. Measurements were carried out for different flow rates at various inclination angles and typical results are presented for $U_{LS} = 0.01$ m/s and $U_{GS} = 0.41$ m/s. The corresponding liquid slug length distributions with bin size of pipe diameter D, are also shown in these figures. For each bin separately, the corresponding trailing bubble velocities were averaged, yielding the ensemble-averaged value $\langle U_{\text{inst}} \rangle$. The standard deviations range between 10% and 50%.

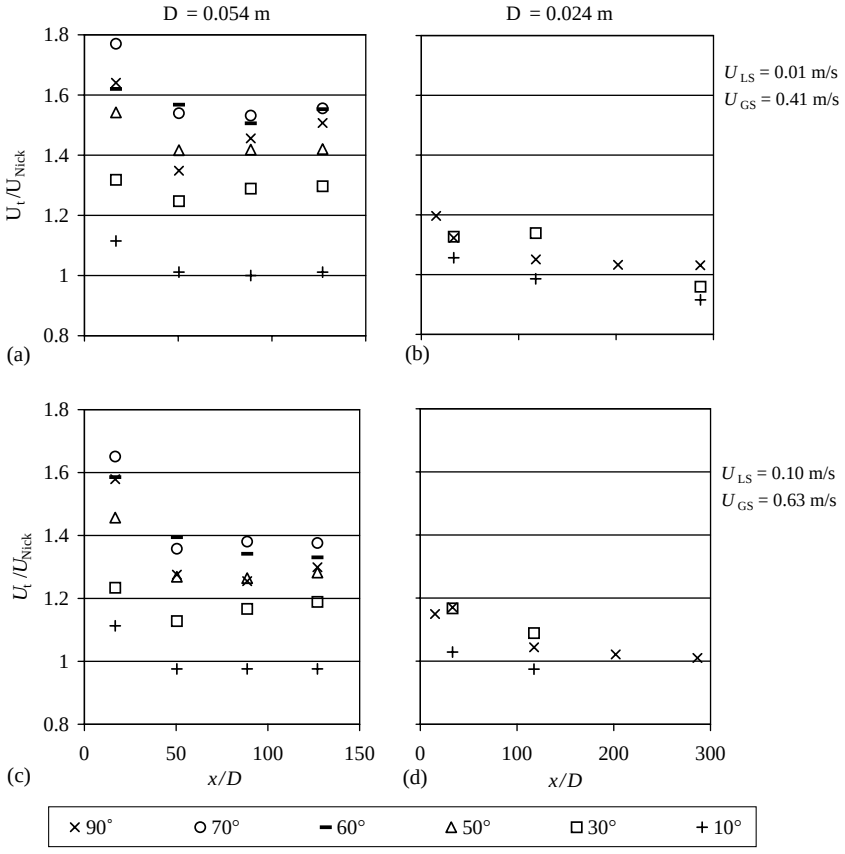

Fig. 1. The characteristic normalized translational velocity according to cross-correlation technique as a function of position along the pipe for different inclination angles and flow rates. $D = 0.054$ and 0.024 m.

Table 1
Translational velocity, U_{Nick} according to Eq. (1), taking gas expansion into account: $D = 0.054$ and 0.024 m

	$U_{LS} = 0.01$ m/s; $U_{GS} = 0.41$ m/s				$U_{LS} = 0.10$ m/s; $U_{GS} = 0.63$ m/s			
$D = 0.054$ m; U_{Nick} (m/s)								
x/D	17	50	89	127	17	50	89	127
90°	0.64	0.66	0.68	0.71	0.95	0.98	1.02	1.07
70°	0.74	0.76	0.79	0.81	1.06	1.09	1.13	1.17
60°	0.79	0.81	0.83	0.85	1.11	1.14	1.17	1.21
50°	0.83	0.84	0.86	0.88	1.16	1.19	1.21	1.24
30°	0.88	0.89	0.90	0.91	1.24	1.25	1.26	1.27
10°	0.87	0.87	0.88	0.88	1.24	1.24	1.25	1.25
$D = 0.024$ m; U_{Nick} (m/s)								
x/D	15	33	118	287	15	33	118	287
90°	0.56	0.57	0.59	0.64	0.87	0.88	0.91	0.99
30°	0.71	0.71	0.72	0.74	1.06	1.06	1.07	
10°	0.71	0.71	0.71	0.71	1.08	1.08	1.08	

The instantaneous velocities are in general characterized by higher values at small separation distances and a constant lower propagation velocity at increasing values of ℓ_s. At $\ell_s < 1D$, just prior to coalescence, both bubbles travel at approximately the same velocity which causes a drop in the approach velocity (Aladjem Talvy et al., 2000). Velocities at large separation distances are well predicted by Eq. (1) for D=0.024 m (Fig. 2), while for the larger diameter pipe (Fig. 3) they are underpredicted (with the exception of $\beta = 10°$). Note that for D=0.054 m (Fig. 3) there exists a large scatter

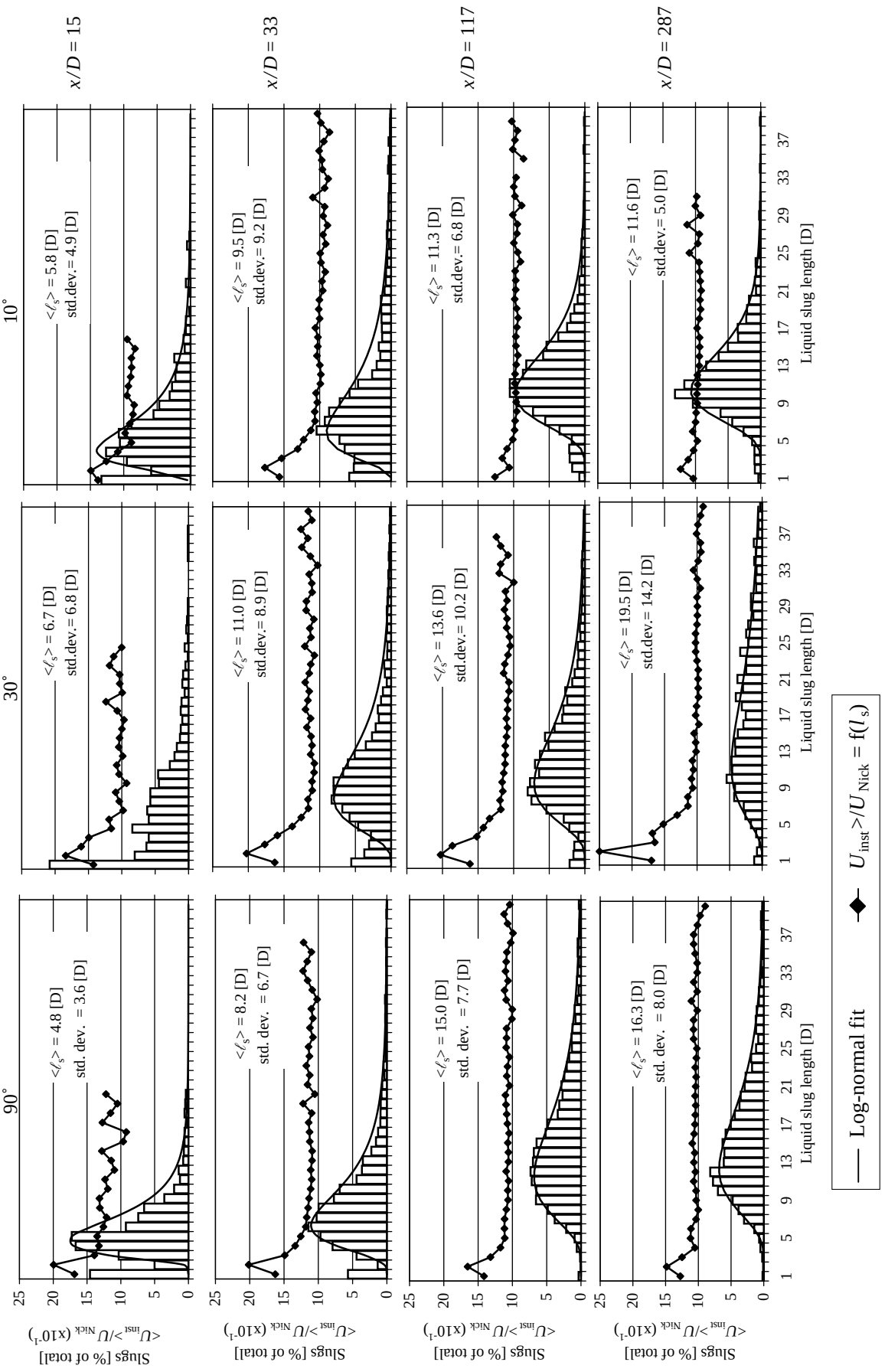

Fig. 2. Instantaneous translational velocity as a function of separation distance and the liquid slug length distribution based on the instantaneous velocity at various positions along the pipe and for different inclination angles: $D = 0.024$ m; $U_{LS} = 0.01$ m/s; $U_{GS} = 0.41$ m/s.

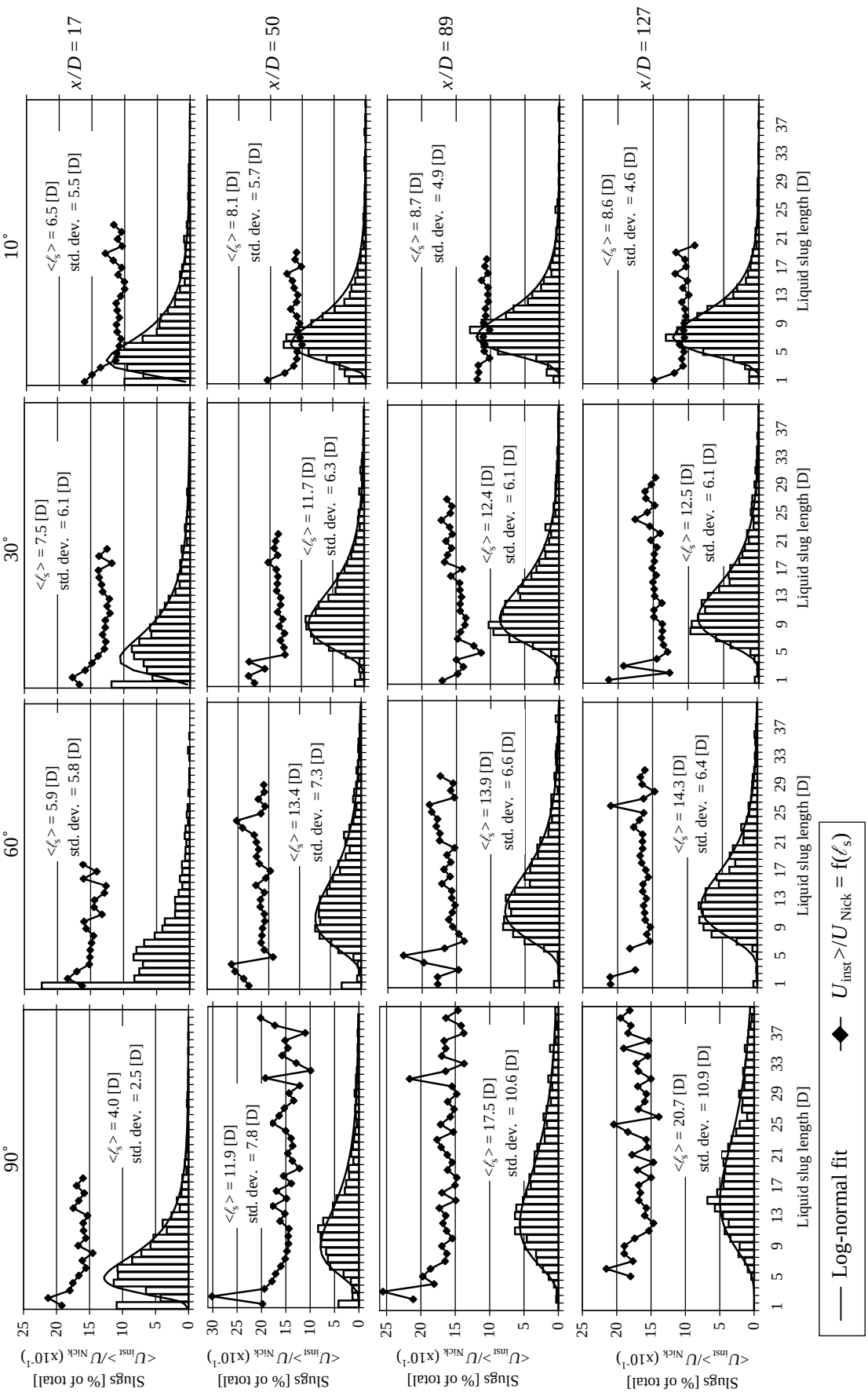

Fig. 3. Instantaneous translational velocity as a function of separation distance and the liquid slug length distribution based on the instantaneous velocity at various positions along the pipe and for different inclination angles: $D = 0.054$ m; $U_{LS} = 0.01$ m/s; $U_{GS} = 0.41$ m/s.

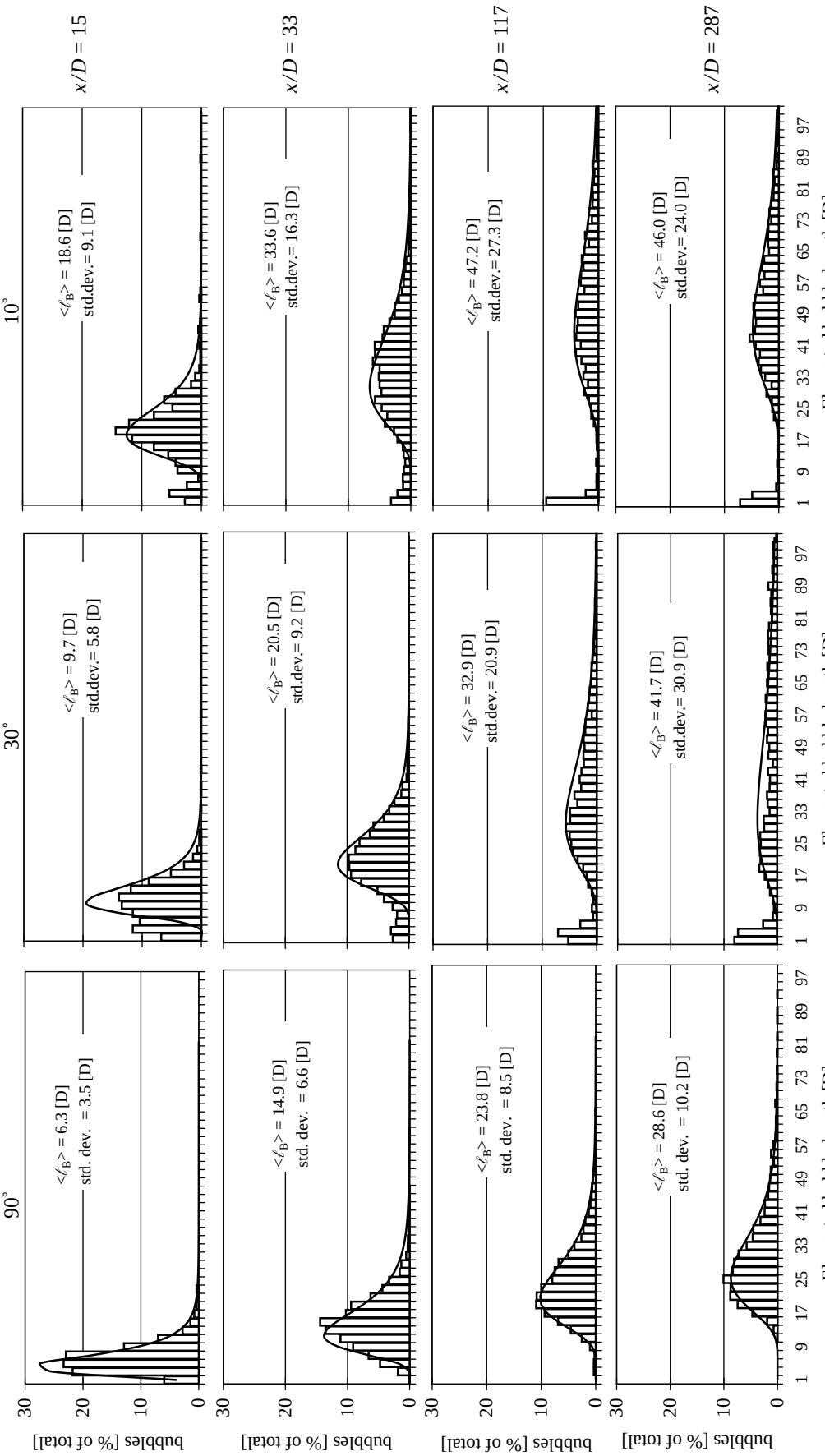

Fig. 4. Elongated bubble length distributions based on the instantaneous velocity at various positions along the pipe and for different inclination angles: $D = 0.024$ m; $U_{LS} = 0.01$ m/s; $U_{GS} = 0.41$ m/s.

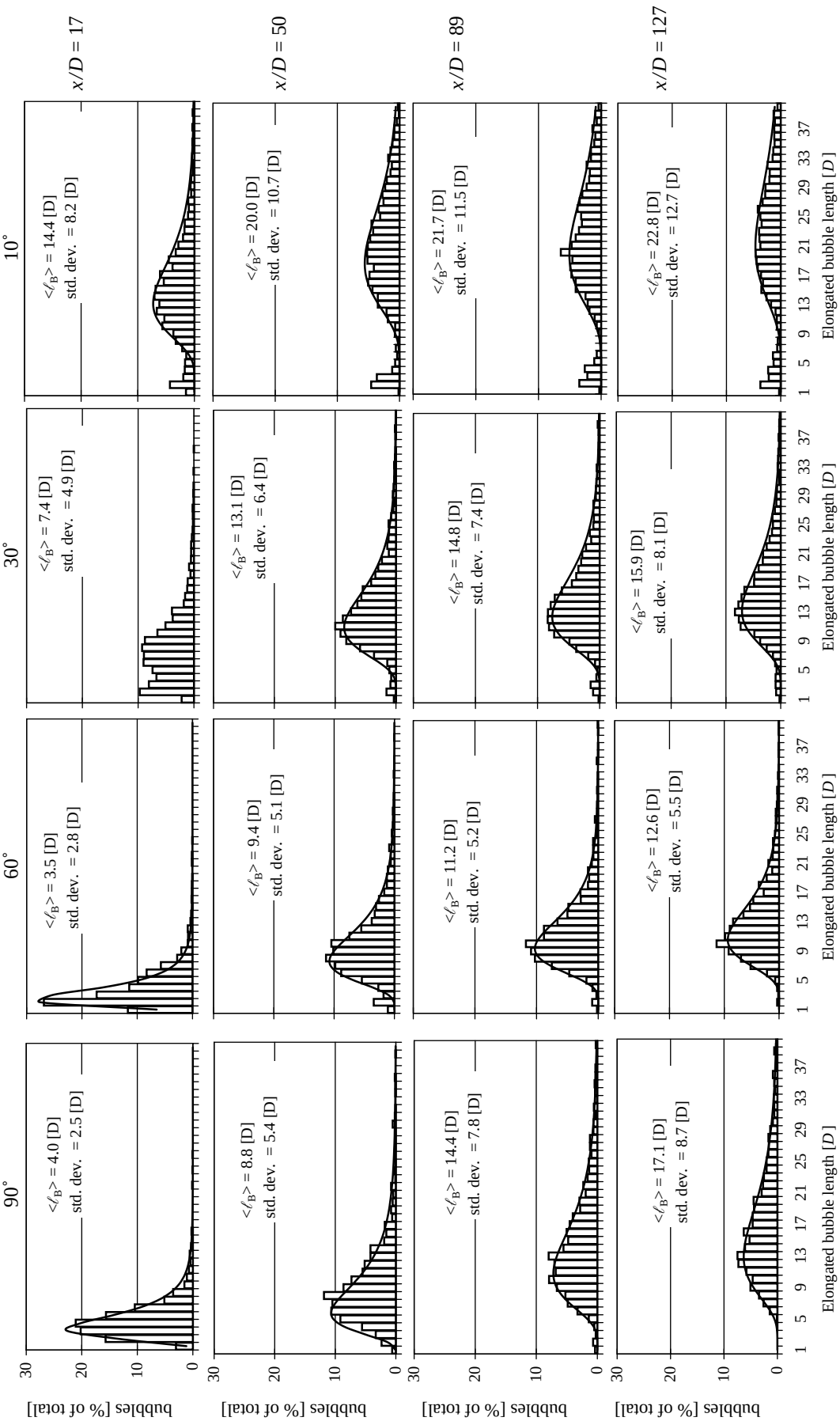

Fig. 5. Elongated bubble length distribution based on the instantaneous velocity at various positions along the pipe and for different inclination angles: $D = 0.054$ m; $U_{LS} = 0.01$ m/s; $U_{GS} = 0.41$ m/s.

Table 2
Parameters ξ and λ of the log-normal fit, Eq. (3). $U_{LS} = 0.01$ m/s; $U_{GS} = 0.41$ m/s

$D = 0.054$ m		Liquid slugs				Elongated bubbles			
x/D		17	50	89	127	17	50	89	127
90°	ξ	1.80	2.38	2.71	2.90	1.27	2.00	2.50	2.72
	λ	0.62	0.53	0.54	0.49	0.56	0.59	0.48	0.46
60°	ξ		2.52	2.55	2.59	0.95	2.17	2.34	2.46
	λ		0.48	0.43	0.40	0.63	0.47	0.41	0.39
30°	ξ	1.90	2.38	2.43	2.43	2.06	2.51	2.64	2.71
	λ	0.72	0.46	0.45	0.45	0.47	0.42	0.41	0.41
10°	ξ	1.73	2.00	2.08	2.08	2.69	3.03	3.10	3.17
	λ	0.71	0.53	0.46	0.45	0.40	0.37	0.38	0.39
$D = 0.024$ m									
x/D		15	33	118	287	15	33	118	287
90°	ξ	1.54	1.98	2.58	2.63	1.69	2.59	3.10	3.35
	λ	0.55	0.59	0.49	0.46	0.56	0.48	0.37	0.34
30°	ξ	2.12	2.34	2.51	2.79	2.34	3.04	3.57	3.77
	λ	0.56	0.56	0.52	0.63	0.43	0.35	0.44	0.60
10°	ξ	1.68	2.11	2.39	2.41	2.96	3.53	3.91	3.92
	λ	0.65	0.67	0.40	0.36	0.35	0.38	0.39	0.36

in the data, especially for $\beta > 30°$. This can be attributed to insufficient ensemble sizes at both large and small separation distances, as well as to the inherently more complex behavior of the flow in the larger pipe diameter.

The evolution of the measured liquid slug and elongated bubble length distributions according to the instantaneous translational velocity, U_{inst}, is shown in Figs. 2–5 for both pipe diameters. In general, the mean and the mode of the length distributions, as well as the standard deviation, increase along the pipe. In all cases both the liquid slug and the elongated bubble length distributions are right-skewed (tails extending to large values). The log-normal shape was fitted to the measured distributions and is depicted in Figs. 2–5 as a solid line. The probability density function of the log-normal distribution (see, e.g. Miller & Freund, 1965) is

$$f(z) = \frac{1}{\sqrt{2\pi}\lambda}\left(\frac{\ell_s}{D}\right)^{-1} \exp - \frac{1}{2}\left[\frac{\ln(\ell_s/D) - \xi}{\lambda}\right]^2 \qquad (3)$$

with $z > 0$ and $\lambda > 0$. The parameters ξ and λ in Eq. (3) are given in Table 2.

The shape and development of the liquid slug length distributions (Figs. 2 and 3) are hardly affected by the pipe diameter whereas the elongated bubble length distributions (Figs. 4 and 5) extend to much larger values for the small pipe.

The effect of the inclination angle on the measured liquid slug and elongated bubble length distributions near the pipe exit is shown in Fig. 6 for $D = 0.054$ m, $U_{LS} = 0.10$ m/s and $U_{GS} = 0.63$ m/s. The mean and the most probable (mode) liquid slug lengths decrease with decreasing β, and the distributions become more peaked with decreasing standard deviations. Contrary to that, the mean and the most probable elongated bubble lengths as well as the standard deviations, exhibit a minimum at $\beta = 60°$. Mean values at 10° are larger than at 90°. Comparing Figs. 3 and 5 with Fig. 6, it can be seen that the shape of both the liquid slug and elongated bubble length distributions near the pipe exit are very similar for both flow rates.

The accumulated data on $\langle U_{\text{inst}}\rangle/U_{\text{Nick}}$ as a function of the liquid slug length ahead of the bubble was averaged over the different measurement positions for each flow rate and inclination angle. The results are presented in Figs. 7 and 8 for $D = 0.024$ and 0.054 m, respectively. It can be seen that for the large pipe (Fig. 8) the maximum normalized approach velocity (at $\ell_s \approx 2D$) decreases with decreasing inclination angle for the same mixture velocity.

The data in Fig. 7 for different flow rates collapse on a single curve and approach the value suggested by Eq. (1) at sufficiently large separation distances. The accumulated data were best-fitted adopting the curve suggested by Moissis and Griffith (1962) with some modifications

$$\frac{U_t}{U_{\text{Nick}}} = a + b\exp(-c\ell_s/D) + \frac{1}{(\ell_s/D)^d}. \qquad (4)$$

The coefficient a represents the normalized elongated bubble translational velocity at large separation distances. The last term, which is absent in the original Moissis and Griffith correlation, is added to account for the slower decay in the translational velocity of elongated bubbles behind relatively long slugs (Aladjem Talvy et al., 2000).

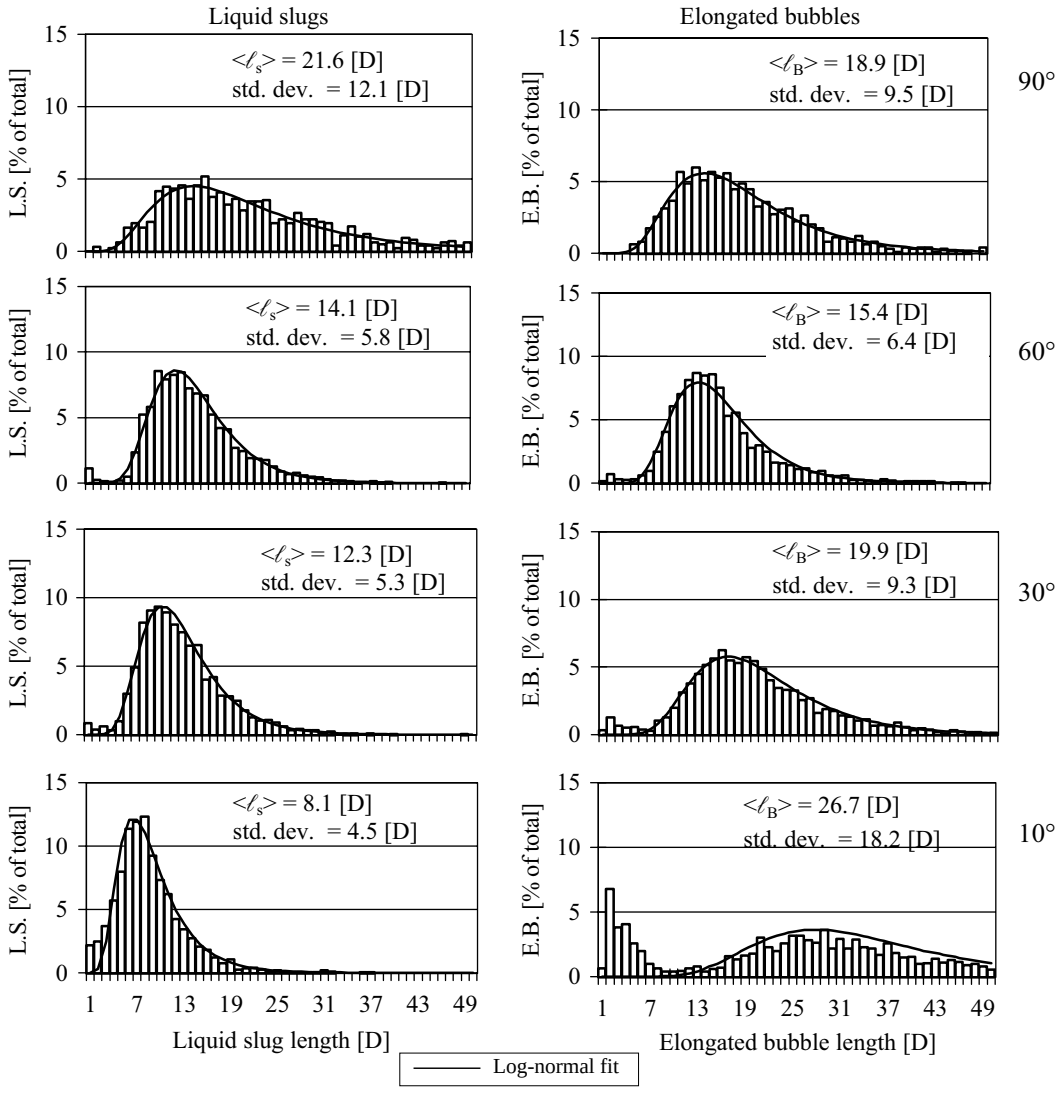

Fig. 6. Liquid slug and elongated bubble length distributions based on the instantaneous velocity at various inclination angles: $D = 0.054$ m; $x/D = 127$; $U_{LS} = 0.10$ m/s; $U_{GS} = 0.63$ m/s.

The pattern observed for the larger pipe in Fig. 8 is much more complicated. The translational velocities do not attain the value predicted by Eq. (1), with the exception of $\beta = 10°$ (Fig. 8(d)), see also van Hout et al. (2002). The effect of the flow rate is also more pronounced in this case, and the data do not collapse on a single curve, as in Fig. 7. The coefficients of the best-fitted curves which express the relation between the elongated bubble nose velocity and the liquid slug length ahead of its nose are given in Fig. 7. These relations dictate the evolution of slug flow along the pipe and are used to predict the length distributions along the pipe using the model of Barnea and Taitel (1993). Fig. 9 presents a comparison between the predicted and the measured liquid slug length distributions for $D = 0.024$ m, $U_{LS} = 0.01$ m/s, $U_{GS} = 0.41$ m/s. In general there is a good agreement between the development and the shape of the predicted and the measured distributions for all inclination angles. However, predicted distributions tend to become more widespread near the pipe exit ($x/D = 287$) and the mean and the mode are slightly overpredicted.

3.3. Mean liquid slug and elongated bubble lengths

Figs. 10 and 11 present the evolution of the dimensionless mean liquid slug and elongated bubble lengths as a function of inclination angle for the two pipe diameters and for various flow rates. In general, the mean lengths increase at a fast rate near the pipe inlet and at a decreasing rate further along the pipe. The normalized mean slug lengths only weakly depend on the flow rates and the pipe diameter. In all cases, the values of $\langle \ell_s \rangle$ are approximately $5D$ near the pipe entrance and increase to 10–20D near the pipe exit. The evolution of the slug length along the pipe depends on the inclination angle. For $\beta = 90°$ the rate of increase is the

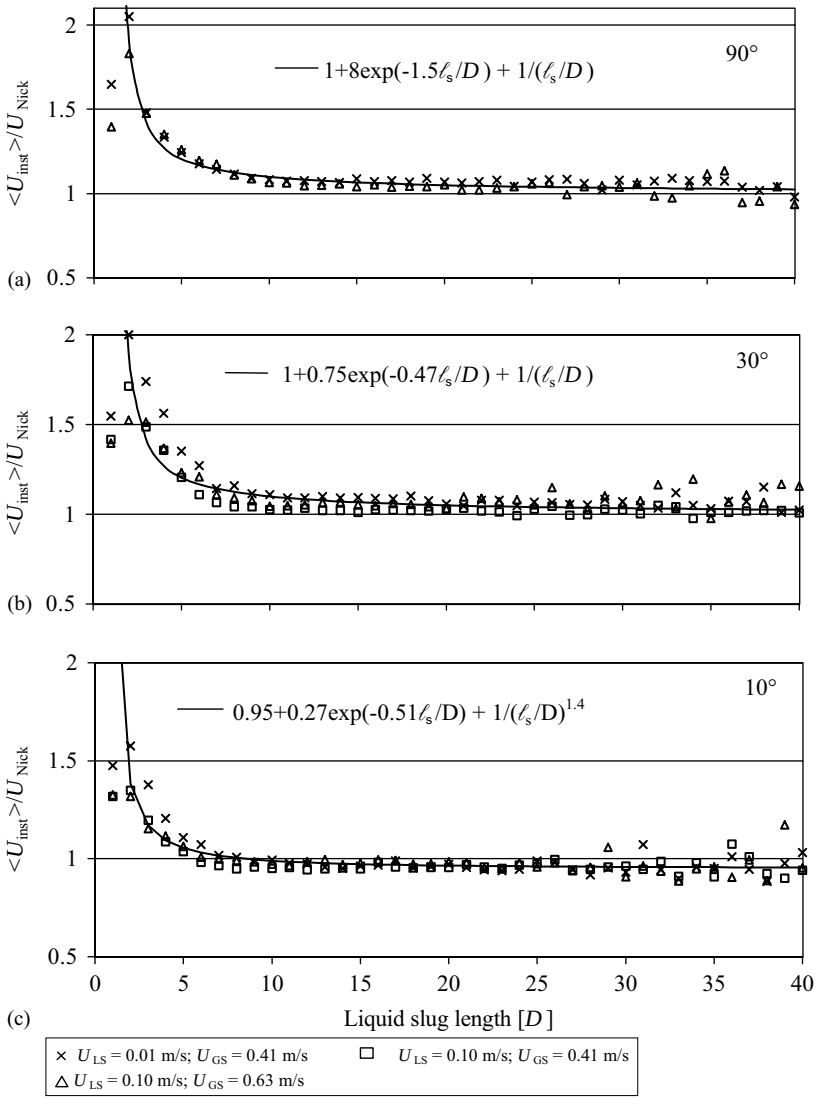

Fig. 7. Averaged instantaneous translational velocity as a function of separation distance for different inclination angles and various flow rates: $D = 0.024$ m.

highest, resulting in longer slugs at the pipe exit. The mean liquid slug lengths at the exit decrease with decreasing inclination angles.

Contrary to $\langle \ell_s \rangle$, the dimensionless mean elongated bubble lengths $\langle \ell_B \rangle$ strongly depend on both the flow rates and the pipe diameter (Fig. 11). This dependency has been qualitatively explained by van Hout et al. (2001). The values of $\langle \ell_B \rangle$ depend on the pipe inclination as well, with the longest bubbles observed at the smallest inclination.

The mean liquid slug and elongated bubble lengths deduced from the optical probe measurements were verified against video images of the flow close to the pipe exit. The results are presented in Fig. 12 for $D = 0.054$ and 0.024 m. The standard deviation ranges from 30% to 60% for the optical probes and from 15% to 50% for the image processing. In general there is a good agreement between the mean lengths obtained by the two methods.

For the large pipe, there is a clear trend of increasing mean liquid slug length with increasing β at a constant flow rate (Figs. 12(a) and (b)). Contrary to that, the highest values of the elongated bubble length are attained at small inclinations. Minimal values of $\langle \ell_B \rangle$ are found between $50° < \beta < 70°$ (Figs. 12(e) and (f)). Measurements in the small pipe between 30° and 90° are absent due to the occurrence of flow pattern instabilities (severe slugging) at these inclination angles and results are therefore inconclusive.

3.4. Slug frequency

The slug frequency ν is defined as the total number of slugs sampled, N, divided by the sampling duration t_s,

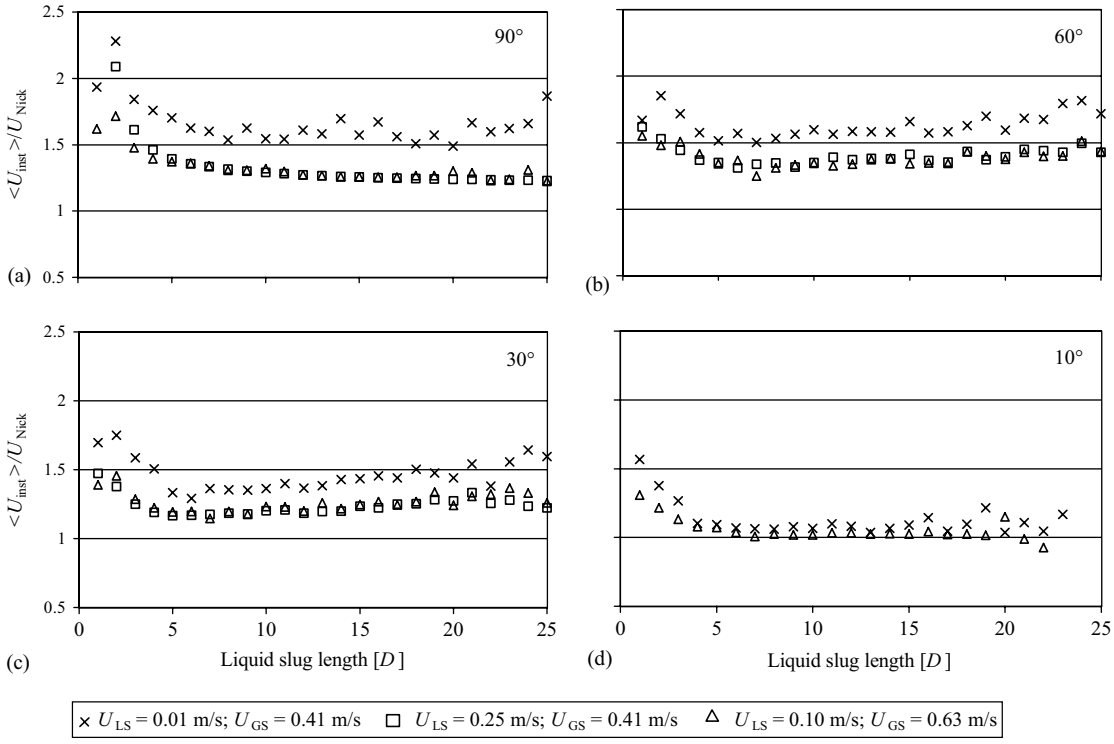

Fig. 8. Averaged instantaneous velocity as a function of the liquid slug length for different inclination angles and various flow rates: $D = 0.054$ m.

$v = N/t_s$. Several thousands of slug units were sampled for each set of experimental conditions. The variation of the slug frequency along the pipe is depicted in Fig. 13 for both pipe diameters, various pipe inclinations and two flow rates. The coalescence rate, which is represented by the variation of the slug frequency along the pipe is high near the entrance of the pipe and decreases towards the end of the pipe. The variation of the coalescence rate essentially defines the extent of the entrance length of slug flow. In all cases this rate remains quite high, up to approximately $x/D = 60$. It should be noted however, that although the extent of the entrance length is hardly affected by the pipe inclination, the initial coalescence rate in the entrance region clearly decreases with decreasing β and has a maximum for $50° < \beta < 70°$ (Figs. 13(a) and (b)).

The slug frequency at the pipe exit as a function of the inclination angle for $D = 0.054$ m is depicted in Fig. 14 for different flow rates. The slug frequency clearly depends on the flow rates and in all cases has a maximum that lies between 50° and 70°. Note that the slug frequency is directly related to the mean length of a slug unit $\ell_u = \ell_B + \ell_s$ and its mean translational velocity. As was shown in Fig. 12, $\langle \ell_s \rangle$ slightly increases with increasing pipe inclination and only weakly depends on flow rate. The slug unit length ℓ_u is therefore mainly determined by ℓ_B. The mean elongated bubble length has a minimum value at approximately 60° (Fig. 12) and strongly depends on the flow rate. The measured translational velocities of elongated bubbles depend on the inclination angle and also have a maximum value at approximately 60° (van Hout et al., 2002). Therefore, at this inclination, relatively short slug units that propagate at high velocities are observed, leading to correspondingly high slug frequencies.

4. Summary and conclusions

An experimental study of the evolution of continuous slug flow along inclined pipes with internal diameters of 0.024 and 0.054 m is presented. The reported hydrodynamic and statistical parameters include liquid slug and elongated bubble length distributions, instantaneous velocities of elongated bubbles as a function of the liquid slug length ahead of it, $U_t = f(\ell_s)$, as well as the evolution of the slug frequency. The measurements were carried out by optical fiber probes at different positions along the pipe. The probe measurements were validated by image processing technique.

Measured length distributions were peaked near the pipe inlet and more widespread with increasing standard deviation further down the pipe. For all cases, measured length distributions were well described by the log-normal shape. The best-fitted curves of $U_t = f(\ell_s)$ for different inclination angles were used as input relation to the model of Barnea and Taitel (1993) for the

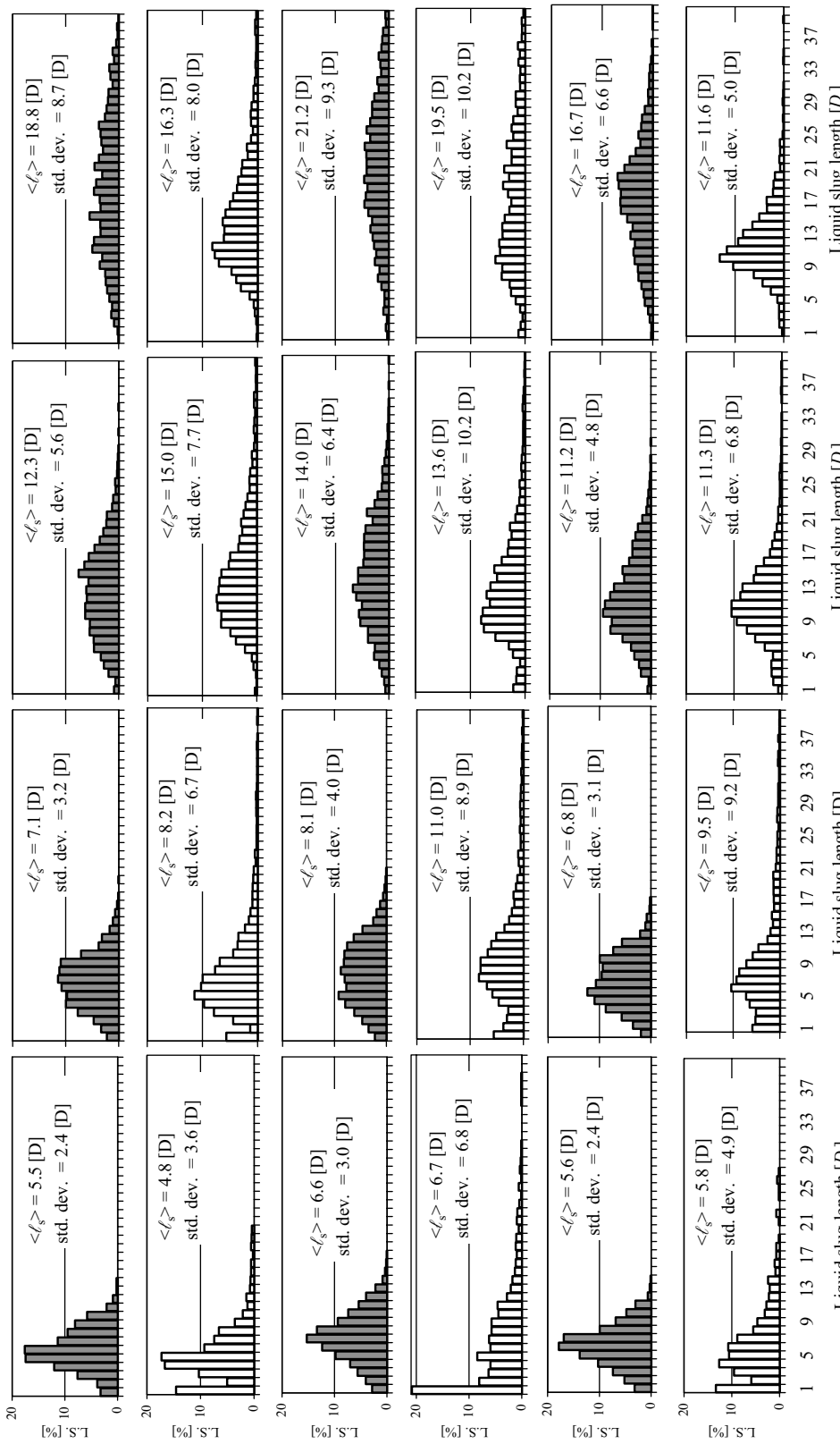

Fig. 9. Comparison between the evolution of the measured and the predicted liquid slug length distributions along the pipe for different inclination angles. $U_{LS} = 0.01$ m/s; $U_{GS} = 0.41$ m/s; $D = 0.024$ m.

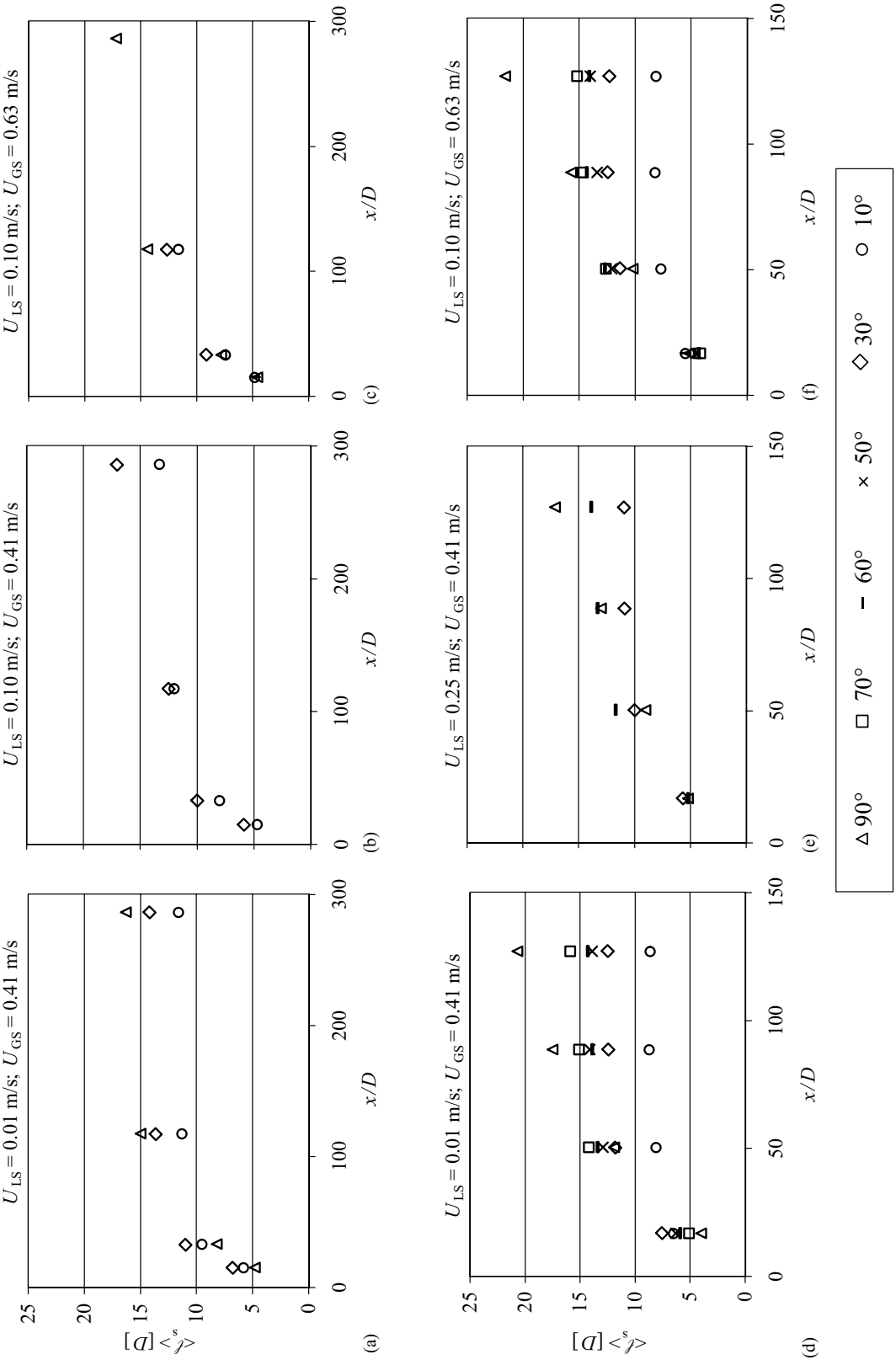

Fig. 10. Mean liquid slug length as a function of position along the pipe for different inclination angles and various flow rates.

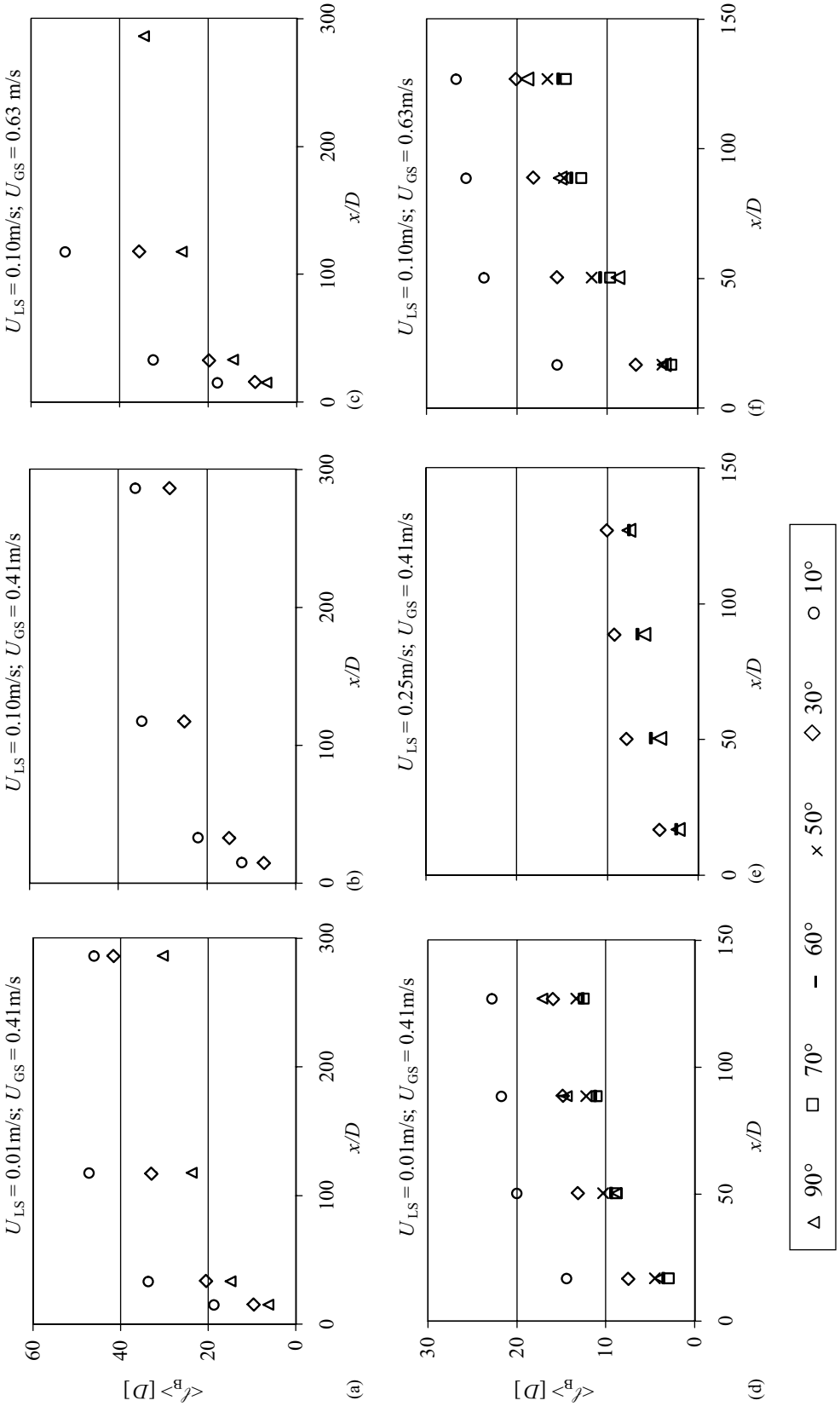

Fig. 11. Mean elongated bubble length as a function of position along the pipe for different inclination angles and various flow rates, $D = 0.024$ and 0.054 m.

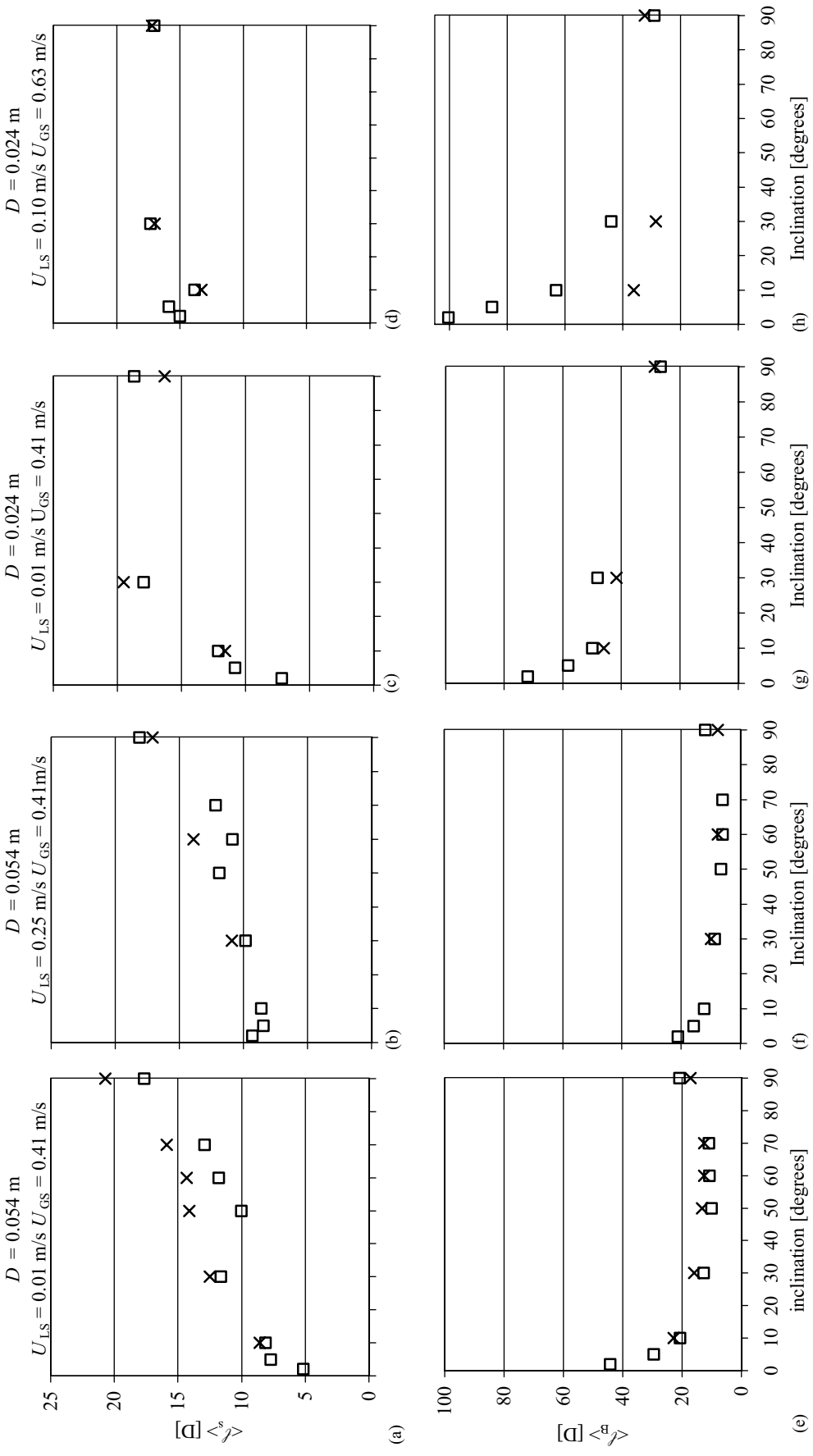

Fig. 12. Mean liquid slug and elongated bubble lengths as a function of the inclination angle for various flow rates near the pipe exit, $D = 0.054$ and 0.024 m.

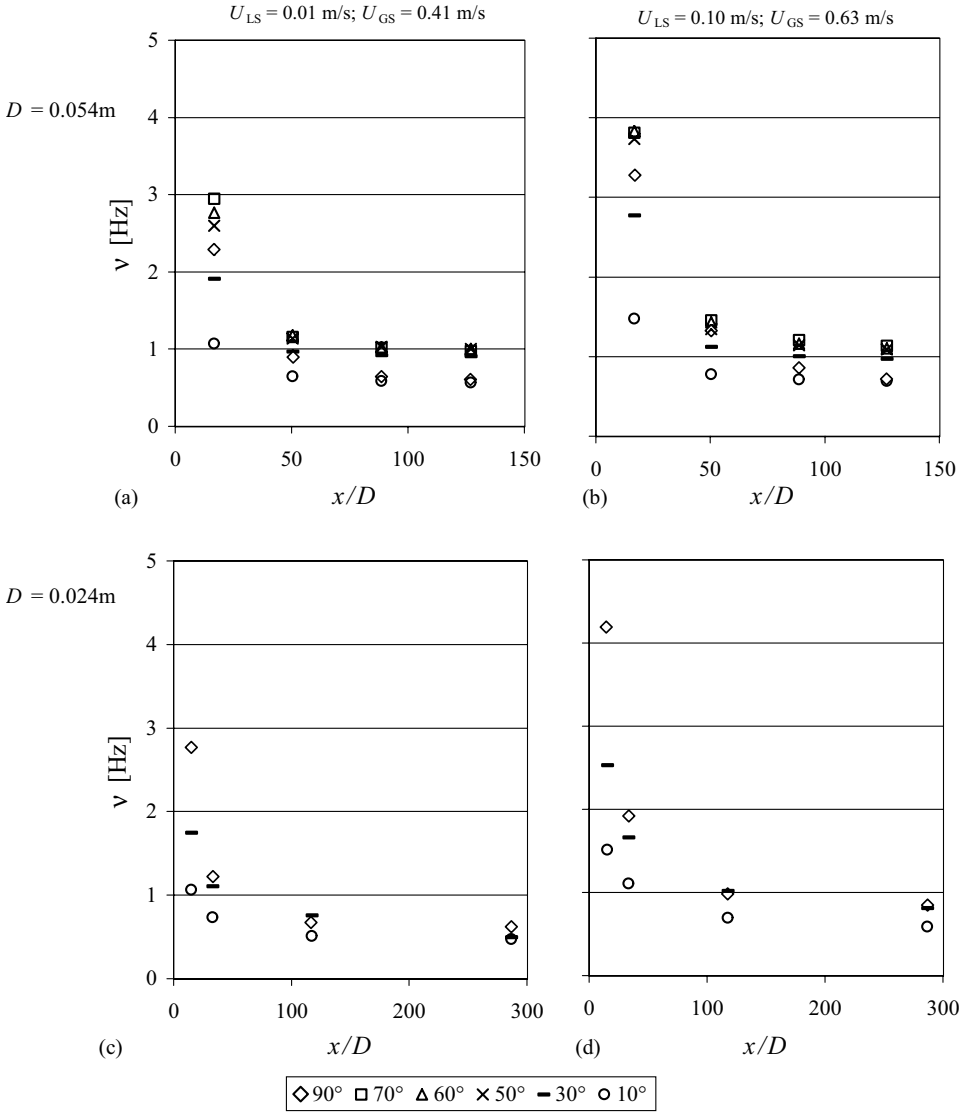

Fig. 13. The slug frequency as a function of position along the pipe for different inclination angles and flow rates.

prediction of the evolution of the length distributions along the pipe. Model predictions and measurements agree well.

For the large pipe, the mean liquid slug lengths at the pipe exit, slowly increase with increasing inclination angle from $5D$–$10D$ at 2° to $10D$–$20D$ at 90° and are only weakly influenced by the current range of pipe diameters and flow rates. In contrast, the dimensionless mean elongated bubble lengths at the pipe exit exhibited a minimum at approximately 60°.

The slug frequency has a maximum between $50° < \beta < 70°$ ($D = 0.054$ m) and its dependency on flow rates, pipe diameter and pipe inclination is closely related to the velocity of a slug unit and the elongated bubble length. The coalescence rate becomes negligible for $x/D > 60$ independent of pipe inclination, flow rates and pipe diameter.

Notation

a, b, c, d	coefficients, Eq. (4)
C	parameter, Eq. (1)
D	internal pipe diameter, m
g	gravitational constant, m/s^2
ℓ_B	elongated bubble length, m
ℓ_s	liquid slug length, m
ℓ_u	length of slug unit, m
N	ensemble size
t_s	sampling duration, s
U_d	drift velocity, m/s
U_{GS}	gas superficial velocity, m/s
U_{inst}	instantaneous propagation velocity of elongated bubble, m/s
U_{LS}	liquid superficial velocity, m/s

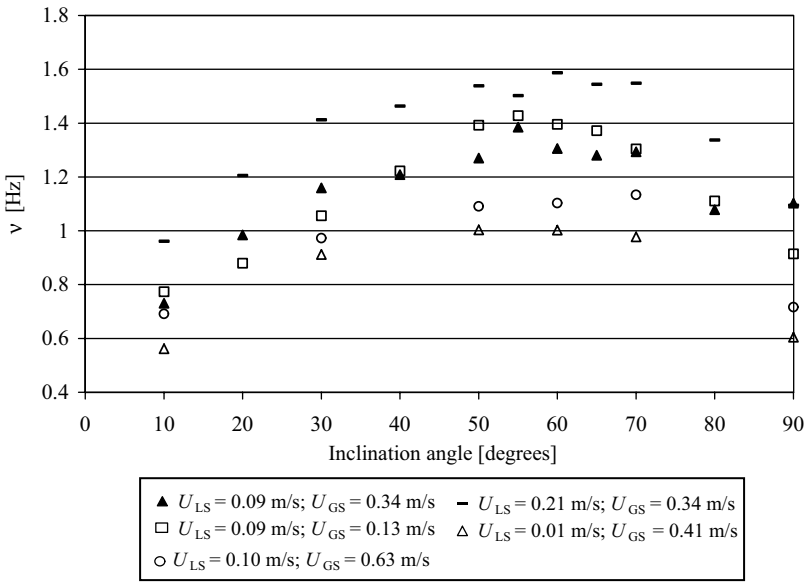

Fig. 14. Slug frequency as a function of pipe inclination near the pipe outlet, $x/D = 127$; $D = 0.054$ m.

U_m mixture velocity, m/s
U_{max} maximum velocity, m/s
U_{Nick} translational velocity according to Eq. (1) m/s,
U_t translational velocity, m/s
x axial coordinate along the pipe, measured from the inlet section, m
y radial distance measured from inner upper pipe wall, m
z variable, Eq. (3)

Greek letters

α_B void fraction in elongated bubble region
β inclination angle, measured from the horizontal, deg
$\Delta\rho$ density difference between liquid and gas phase, kg/m^3
ξ, λ parameters of log-normal distribution, Eq. (3)
σ surface tension,
Σ surface tension parameter
ν slug frequency

Superscripts

h horizontal
v vertical

Other

$\langle .. \rangle$ mean value

Acknowledgements

This work was partially supported by a grant from the Israel Science Foundation. The authors gratefully acknowledge this support.

References

Aladjem Talvy, C., Shemer, L., & Barnea, D. (2000). On the interaction between two consecutive elongated bubbles in a vertical pipe. *International Journal of Multiphase Flow*, *26*, 1905–1923.

Andreussi, P., Bendiksen, K. H., & Nydal, O. J. (1993). Void distribution in slug flow. *International Journal of Multiphase Flow*, *19*, 817–828.

Barnea, D. (1990). Effect of bubble shape on pressure drop calculations in vertical slug flow. *International Journal of Multiphase Flow*, *16*, 79–89.

Barnea, D., & Shemer, L. (1989). Void fraction measurement in vertical slug flow: Applications to slug characteristics and transitions. *International Journal of Multiphase Flow*, *15*, 495–504.

Barnea, D., & Taitel, Y. (1993). A model for slug length distribution in gas–liquid slug flow. *International Journal of Multiphase Flow*, *19*, 829–838.

Bendiksen, K. H. (1984). An experimental investigation of the motion of long bubbles in inclined tubes. *International Journal of Multiphase Flow*, *10*, 467–483.

Benjamin, T. B. (1968). Gravity currents and related phenomena. *Journal of Fluid Mechanics*, *31*, 209–248.

Bernicot, M., & Drouffe, J. M. (1989). Slug length distribution in two-phase transportation systems. *Proceedings of the fourth international conference on multiphase flow*, Nice, France, BHRA, Cranfield, Beds (pp. 485–493).

Brill, J. P., Schmidt, Z., Coberly, W. A., Herring, J. D., & Moore, D. W. (1981). Analysis of two-phase tests in large-diameter flow lines in prudhoe bay field. *Society of Petroleum Engineers Journal*, *271*, 363–378.

Carew, P. S., Thomas, N. H., & Johnson, A. B. (1995). A physically based correlation for the effects of power law rheology and inclination on slug bubble rise velocity. *International Journal of Multiphase Flow*, *21*, 1091–1106.

Cook, M., & Behnia, M. (2000). Slug length prediction in near horizontal gas–liquid intermittent flow. *Chemical Engineering Science*, *55*, 2009–2018.

Costigan, G., & Whalley, P. B. (1997). Slug flow regime identification from dynamic void fraction measurements in vertical air–water flows. *International Journal of Multiphase Flow*, *23*, 263–282.

Dhulesia, H., Bernicot M., & Deheuvels, P. (1991). Statistical analysis and modelling of slug lengths. *Proceedings of the fifth international conference on multiphase production*, Cannes, France, BHRA, Cranfield, Beds (pp. 80–112).

Dumitrescu, D. T. (1943). Strömung an einer Luftblase im senkrechten Rohr. *Zeitschrift für Angewandte Mathematik and Mechanik*, *23*, 139–149.

Fabre, J., & Liné, A. (1992). Modeling of two-phase flow. *Annual Review of Fluid Mechanics*, *24*, 21–46.

Fagundes Netto, J. R., Fabre, J., Grenier, P., & Péresson, L. (1998). An experimental study of an isolated long bubble in an horizontal liquid flow. *Proceedings of the third international conference on multiphase flow*, ICMF'98, Lyon, France, June 8–12.

Felizola, H., & Shoham, O. (1995). A unified model for slug flow in upward inclined pipes. *Journal of Energy Resources Technology*, *117*, 7–12.

Griffith, P., & Wallis, G. B. (1961). Two-phase flow. *Journal of Heat Transfer*, *83*, 307–320.

Hasan, A. R., & Kabir, C. S. (1986). Predicting multiphase flow behavior in a deviated well. *61st annual technical conference*, New Orleans, LA, SPE 15449.

Hasanein, H. A., Tudose, G. T., Wong, S., Malik, M., Esaki, S., & Kawaji, M. (1996). Slug flow experiments and computer simulation of slug length distribution in vertical pipes. *A.I.Ch.E. symposium series heat transfer*, Houston.

van Hout, R., Barnea, D., & Shemer, L. (2001). Evolution of statistical parameters of gas–liquid slug flow along vertical pipes. *International Journal of Multiphase Flow*, *27*, 1579–1602.

van Hout, R., Barnea, D., & Shemer, L. (2002). Translational velocities of elongated bubbles in continuous slug flow. *International Journal of Multiphase Flow*, 28, 1333–1350.

van Hout, R., Shemer, L., & Barnea, D. (1992). Spatial distribution of void fraction within the liquid slug and some other related slug parameters. *International Journal of Multiphase Flow*, *18*, 831–845.

Miller, I., & Freund, J. E. (1965). *Probability and statistics for engineer*. Englewood Cliffs, NJ: Prentice-Hall.

Moissis, R., & Griffith, P. (1962). Entrance effects in a two-phase slug flow. *Journal of Heat Transfer*, *84*, 366–370.

Nicholson, M. K., Aziz, K., & Gregory, G. A. (1978). Intermittent two phase flow in horizontal pipes: Predictive models. *The Canadian Journal of Chemical Engineering*, *56*, 653–663.

Nicklin, D. J., Wilkes, J. O., & Davidson, J. F. (1962). Two-phase flow in vertical tubes. *Transactions of the Institute of Chemical Engineers*, *40*, 61–68.

Nydal, O. J., Pintus, S., & Andreussi, P. (1992). Statistical characterization of slug flow in horizontal pipes. *International Journal of Multiphase Flow*, *18*, 439–453.

Pinto, A. M. F. R., & Campos, J. B. L. M. (1996). Coalescence of two gas slugs rising in a vertical column of liquid. *Chemical Engineering Science*, *51*, 45–54.

Pinto, A. M. F. R., Coelho Pinheiro, M. N., & Campos, J. B. L. M. (1998). Coalescence of two gas slugs rising in a co-current flowing liquid in vertical tubes. *Chemical Engineering Science*, *53*, 2973–2983.

Polonsky, S., Shemer, L., & Barnea, D. (1999). The relation between the Taylor bubble motion and the velocity field ahead of it. *International Journal of Multiphase Flow*, *25*, 957–975.

Shemer, L., & Barnea, D. (1987). Visualization of the instantaneous velocity profiles in gas–liquid slug flow. *PhysicoChemical Hydrodynamics*, *8*, 243–253.

Weber, M. E., Alarie, A., & Ryan, M. E. (1986). Velocities of extended bubbles in inclined tubes. *Chemical Engineering Science*, *41*, 2235–2240.

Zukoski, E. E. (1966). Influence of viscosity, surface tension, and inclination angle on the motion of long bubbles in closed tubes. *Journal of Fluid Mechanics*, *25*, 821–837.